(12)

PHOTON-BURST CORRELATION TECHNIQUES FOR ATMOSPHERIC CROSSWIND MEASUREMENTS

FINAL REPORT

C. Y. SHE AND R. F. KELLEY

SEPTEMBER, 1983

U. S. ARMY RESEARCH OFFICE

CONTRACT DAAG29 80 C 0038
(12/14/1979 - 6/13/1983)

DEPARTMENT OF PHYSICS
COLORADO STATE UNIVERSITY
FORT COLLINS, COLORADO 80523

APPROVED FOR PUBLIC RELEASE;
DISTRIBUTION UNLIMITED.

THE VIEW, OPINIONS, AND/OR FINDINGS CONTAINED IN THIS REPORT ARE THOSE OF THE AUTHOR(S) AND SHOULD NOT BE CONSTRUED AS AN OFFICIAL DEPARTMENT OF THE ARMY POSITION, POLICY, OR DECISION, UNLESS SO DESIGNATED BY OTHER DOCUMENTATION.

Unclassified

SECURITY CLASSIFICATION OF THIS PAGE (When Data Entered)

REPORT DOCUMENTATION PAGE

READ INSTRUCTIONS BEFORE COMPLETING FORM

1. REPORT NUMBER	2. GOVT ACCESSION NO. AD-A134617
3. RECIPIENT'S CATALOG NUMBER	
4. TITLE (and Subtitle) Photon-Burst Correlation Techniques for Atmospheric Crosswind Measurements	5. TYPE OF REPORT & PERIOD COVERED Final Report 12/14/79 - 6/13/83
	6. PERFORMING ORG. REPORT NUMBER
7. AUTHOR(s) C. Y. She and R. F. Kelley	8. CONTRACT OR GRANT NUMBER(s) DAAG29-80-C-0038
9. PERFORMING ORGANIZATION NAME AND ADDRESS Colorado State University	10. PROGRAM ELEMENT, PROJECT, TASK AREA & WORK UNIT NUMBERS
11. CONTROLLING OFFICE NAME AND ADDRESS U. S. Army Research Office Post Office Box 12211 Research Triangle Park, NC 27709	12. REPORT DATE September 1983
	13. NUMBER OF PAGES
14. MONITORING AGENCY NAME & ADDRESS(if different from Controlling Office)	15. SECURITY CLASS. (of this report) Unclassified
	15a. DECLASSIFICATION/DOWNGRADING SCHEDULE

16. DISTRIBUTION STATEMENT (of this Report)

Approved for public release; distribution unlimited.

17. DISTRIBUTION STATEMENT (of the abstract entered in Block 20, if different from Report)

18. SUPPLEMENTARY NOTES

The view, opinions, and/or findings contained in this report are those of the author(s) and should not be construed as an official Department of the Army position, policy, or decision, unless so designated by other documentation

19. KEY WORDS (Continue on reverse side if necessary and identify by block number)

Photon-burst correlation
Laser velocimetry
Crosswind measurements
Turbulence induced beam radii

20. ABSTRACT (Continue on reverse side if necessary and identify by block number)

With a cw visible laser, the method of photon-burst correlation is used to measure atmospheric crosswinds. A scaling law, including the effects of atmospheric turbulence, for performance evaluation of both laser Doppler (LDV) and laser time-of-flight (LTV) velocimeters, is introduced theoretically and established experimentally with field experiments. Crosswind measurements in the night at a range of 500 m with a low power argon-ion laser are reported. The measured signal particle arrival rate is consistent with the predicted arrival rate based on the scaling law. In addition to the use of higher laser power, it is suggested (cont)

DD FORM 1 JAN 73 1473 EDITION OF 1 NOV 65 IS OBSOLETE

UNCLASSIFIED

SECURITY CLASSIFICATION OF THIS PAGE (When Data Entered)

20. Abstract (Continued)

cont

that with proper inclusion of signal photon bursts resulting from the simultaneous arrival of several particles, routine operation of this type of laser velocimeter for long ranges, up to 1000 m, should be feasible.

Table of Contents

Statement of the Problem

A three-year research program to investigate the performance and potential of the laser time-of-flight (LTV) velocimeter with photon-burst correlation detection for remote sensing of atmospheric crosswinds.

Summary of Results

i. The scaling law for the performance evaluation of crosswind measurements with visible velocimeters has been established theoretically and confirmed with laboratory and field experiments.

ii. The effects of atmospheric turbulence on laser beam separation and beam radius have been assessed experimentally with a diode array and the results interpreted.

iii. The signal particle arrival rate for crosswind measurements at a range of 500 m has been predicted from the scaling law and the results agreed with the measured rates within the experimental errors.

iv. With the successful measurements at a 500 m range, reported for the first time, it is suggested that with proper method for signal analysis, routine operation of visible laser velocimetry at long ranges, up to 1000 m, should be feasible.

List of Publications

1. C. Y. She and R. F. Kelley, "Scaling Law and Photon-Count Distribution of a Laser Time-of-Flight Velocimeter," J. Opt. Soc. Am. 72, 365 (1982).

2. R. F. Kelley, L. S. Hsu, H. Shimizu, and C. Y. She, "A Scaling Law for Performance Evaluation of a Laser Time-of-Flight Velocimeter," in Photon Correlation Techniques in Fluid Dynamics, E. O. Schulz-DuBois, ed., p. 205 (Springer-Verlag, 1983).

3. H. Shimizu, S. A. Lee, and C. Y. She, "High Spectral Resolution Lidar System with Atomic Blocking Filters for Measuring Atmospheric Parameters," Appl. Opt. 22, 1373 (1983).

4. R. F. Kelley, L. S. Hsu, and C. Y. She, "Effect of Turbulence on the Scaling Law for a Laser Time-of-Flight Velocimeter," submitted to J. Opt. Soc. Am. for publication.

5. C. Y. She and R. F. Kelley, "Photon-Burst Correlation Techniques for Atmospheric Crosswind Measurements," submitted to Applied Physics (Springer-Verlag) for publication.

Scientific Personnel

Chiao-Yao She, Professor of Physics and Principal Investigator,
12/14/79 - 6/13/83

Hiroshi Shimizu, Visitor from Japan Environmental Agency and Investigator,
6/9/81 - 7/31/82

Richard F. Kelley,* Graduate Student and Investigator,
12/14/79 - 6/13/83

Long-Sheng Hsu, Graduate Student and Investigator,
9/1/80 - 6/13/83

John V. Prodan, Graduate Student,
7/1/80 - 12/31/80

David W. Clair, Graduate Student,
1/1/80 - 5/31/80

---

*A Ph.D. thesis in Physics at Colorado State University has been written, entitled, "Performance Evaluation and Estimation of a Laser Time-of-Flight Velocimeter."

I. Introduction

It is well known that the frequency of scattered light from a moving particle is Doppler shifted by an amount proportional to its velocity. This concept was first used in laser light scattering to measure flow velocities in 1964 by Yeh and Cummins [1]. Since that time, variations of their technique have been suggested theoretically and tested experimentally in the laboratory, as well as in the atmosphere, with considerable success. A very recent review by Danielsson and Pike [2] has provided an excellent general account on the history of laser velocimetry, the comparison between coherent and incoherent systems, and the feasibility for long-range atmospheric wind sensing. We concur with the main conclusions of this review that because of the large coherent detection area at 10.6 μm and its high laser efficiency and power, the coherent CO_2 lidar system is most suitable for long-range radial wind velocity measurements, but that when higher spatial resolution is required, laser velocimetry using visible wavelengths with photon correlation analysis still offers the best results for atmospheric crosswind measurements. In addition to aircraft applications, intensive studies for a Global wind measuring satellite system (WINDSAT) based on CO_2 coherent lidar technology are underway [3] and the routine operation of its ground-based prototype system has been reported [4]. On the other hand, although impressive progress in atmospheric crosswind measurements with visible wavelengths and photon correlation has been made [5], further developments and investigations for long-range applications are still needed.

In this report, we first review the progress of atmospheric crosswind measurements in the visible for intermediate ranges (roughly 25 m - 150 m) with the emphasis on photon-burst correlation techniques which we developed for individual particle scattering [6-8]. The effect of atmospheric turbulence on beam radius and on performance evaluation and prediction for long-range applications from the scaling law [9,10] is discussed both theoretically and experimentally. Finally, the prospect for long-range (roughly 150 m - 1000 m) crosswind measurements with cw lasers in the visible wavelengths using photon-burst techniques, perhaps modified to handle the unavoidable multiple particle scattering in these ranges is suggested.

Although quite related to each other, the optical system for crosswind measurements in the visible is commonly classified as the differential Doppler (LDV) and laser transit or time-of-flight (LTV) systems. A brief listing for successful atmospheric crosswind measurements without artificial seeding according to the range and year of the work runs as Bourke and Brown (30 m, 1971 [11]), Farmer and Hornkohl (30 m, 1973 [12]), Bartlett and She (60 m, 1976 [6]), Danielsson (60 m, 1980 [13]), and Durst et al (105 m, 1980 [14]) with LDV, and Bartlett and She (100 m, 1977 [7]) and Lading et al (70 m, 1978 [15]) with LTV. We note that photon correlation is the key to success of all this work. The concept of single-particle scattering and single photon-burst correlation, which is knowingly or unknowingly involved in the crosswind measurements for intermediate ranges, has been the main theme of our work [6-10] and will be reviewed here briefly. We also noticed that more recently, Durst, Howe, and Richter [16] have reported a complete LDV system with automated data acquisition suitable for routine

measurement of crosswind velocity component at intermediate range (106 m). This system, whose data analysis is capable of handling photon bursts resulting from multiple-particle scattering, as well as single particle, may be suitable for applications in longer ranges.

II. Single and Multiple Particle Scattering

Natural aerosol comes in different sizes and at random time intervals. Depending on spatial resolution, incident laser power, and detection system which may be set to partially eliminate weaker background, the signal for a velocity measurement consists of a single or multiple photon burst resulting from single or multiple particle scattering [8]. The performance of LDV and LTV depends on aerosol conditions and the manner in which these photon bursts are analyzed.

Perhaps the simplest way to appreciate the differences between single and multiple particle scattering is to consider several hypothetical situations of light scattering from dust particles, as depicted in Fig. 1. Four different combinations of dust particles are shown to traverse a set of interference fringes on the left and two illuminated laser beams on the right. Case (a) consists of many small particles which scatter an almost constant intensity of light n(t), say, in an arbitrary unit of 10, at all times. The small intensity variation detected in this case is the result of fluctuations of Poisson statistics. As can be seen in case (a), the simultaneous scattering from many small particles at random positions yields no useful speed information. If a single particle big enough to yield a burst of light sufficient for a speed measurement (we shall call it a signal particle) traverses the interference fringes and/or the two illuminated beams, the detected scattering intensity maps out the intensity profile of the viewing volume and provides the information necessary for the wind-speed measurement. As shown in case (b) in Fig. 1, the scattered intensity is much less than the detected background light of case (a), but its temporal variation contains the desired speed information. A physically

very unlikely case is case (c), in which five signal particles are aligned in parallel to the interference fringes and are traversing the viewing volume together. This is very desirable because the contributions of these particles even in the incoherent case add to produce a five-fold increase in the intensity variation for speed measurements. The small fluctuations in intensities in cases (b) and (c) are again statistical. In case (d), 20 randomly distributed signal particles are assumed to traverse the scattering volume. The background light is more intense than that due to one large particle, but the variation in intensity which contains the velocity information is proportionally much less due to interferences resulting from the random positions of these scatterers. As these particles traverse the two illuminated beams, the scattered intensity bursts are much wider, resulting in a partial washout of speed information. It is apparent that the signal-to-noise ratio resulting from the 20 scatterers (case d) is no better than that due to a single signal particle (case b). In fact, as the number of scatterers continue to increase, the visibility of the interference fringes and illuminated beam profiles, as measured by scattered light, would be washed out and the desired speed information no longer contained in the detected light intensity. Therefore the signal for a speed measurement, when feasible, is best provided by the scattering of a large single particle.

Although multiple-particle scattering degrades signal-to-noise for speed measurements as depicted in Fig. 1, a process called clipping used in performing digital correlation [8,17], which eliminates the background of case (d) in Fig. 1, will enhance the signal-to-noise considerably unless the number of scatterers is truly overabundant, as depicted in case (a) of Fig. 1. Therefore, a photon burst, resulting from

simultaneous scattering from a few particles, when properly processed is also useful for speed measurement. Such a photon burst can be important and should be included when long-range crosswind measurements are considered.

III. The Photon Burst Correlation Method

To gain some feeling about the typical photon burst sizes encountered in a crosswind measurement, we consider the signal from a dust particle 2 μm in diameter backscattered from a 0.1 W, 0.5 cm diameter laser beam at a distance of 20 m from the detector. The back-scattering differential cross-section [18] is approximately $0.2\ r^2$ where r is the radius of the particle. Since the laser intensity is $0.5\ W/cm^2$, the differential back-scattered power would be $(0.5)(0.2)(1 \times 10^{-4})^2 = 1.0 \times 10^{-9}$ W/sr. With a 20 cm diameter receiving telescope, the detection solid angle is 7.85×10^{-5} sr. For a laser at 5145 Å and a photomultiplier tube with 20 per cent quantum efficiency, the detected photon rate is calculated to be 4×10^4 counts per second. If the particle's transverse velocity is 100 cm/s, it stays in the 0.5 cm beam for 5 ms, giving rise to a total detection of 200 photon counts. This is quite adequate for obtaining a single-burst digital correlation to determine wind speed. In practice, more than 0.1 W of power could be used to enhance the desired single-particle signal for measurements at intermediate ranges. At long ranges (>150 m), photon bursts resulting from multiple-particle scattering should also be considered.

The photon burst signal is analyzed by a digital correlator, in which time is divided into discrete sample times, τ_o and the number of photon counts, $n(i)$ in each sample time is measured. The digital correlation function of this signal for a sequence of N samples is defined as

$$R(\tau) = R(j\tau_o) = \sum_{i=j}^{N} n(i)n(i-j) \qquad (1)$$

where $1 \leq j \leq J$ and J is the maximum number of delay channels in the correlator. To speed up the computation of $R(\tau)$, a process called single clipping [17] is often used. In this method, n(i-j) is set to either 1 or 0 in a shift register depending on whether or not the actual n(i-j) is greater than κ, a preset integer called the clip level. The time-consuming multiplication in (1) can then be done by first anding each pulse of the present sample n(i) with the shift register contents and then accumulating the results in the memory stores, to form $R(\tau)$ in real time. When a relatively large photon burst is analyzed, n(i) exceeds the clip level in most samples during the burst so that n(i-j) = 1; the single-clipped correlation function, extrapolated to R(0) at $\tau = 0$, gives, at least approximately, the total number of counts in the photon burst. The size of the photon burst (in counts) can then be read directly from the correlation function at $\tau = 0$ as R(0) minus the noise background.

The experimental arrangement utilized in the LTV field measurements is shown in Fig. 2. The output of a 1.5 W cw argon-ion laser at 5145 Å is sent to a Malvern model RF307 beam splitter. Using a single telescope, the two beams from the beam splitter are focussed at the sensing volume. The scattered light is collected by a Celestron 8-inch Schmidt-Cassegrain receiving telescope and detected by a ITT FW130 photomultiplier operated as a photon counter. The detected photon bursts are sent to a Malvern K7023 digital correlator and a HP85 computer for analysis. The wind speed is also measured by a cup anemometer with associated electronics. The fan, indicated in Fig. 2, is used for the laboratory experiments only. For our initial LDV field experiment [6], the focussing telescope was removed and the two beams were made to cross at the sensing volume forming intensity interference fringes. For field experiments to verify

the scaling law, the beam splitter was removed and one laser beam was focussed to a spot in the sensing volume. The setup for indoor laboratory experiments [9,10] is similar except that the focussing and receiving telescopes were replaced by simple lenses, and the wind was created by a fan running at a constant speed.

Before conducting serious studies of laser velocimetry, the above setup was used to clarify the sensitivity of the photon-burst method, and determine the minimum detectable burst counts. For this purpose, many LTV and LDV speed measurements under minimal stray light conditions were made in the laboratory. Six selected resulting correlation functions are shown in Fig. 3. Figure 3(a) corresponds to a particle just big enough for a LTV speed measurement. Although the signal-to-noise is not great, two humps are clearly discernable. The total signal count of the photon burst is seen to be less than 10 counts. Figure 3(b) represents background noise which has been somewhat reduced by the preset clipping level. Figure 3(c) depicts a beautiful LTV correlation function from which particle speed can be determined accurately. Even for this high level of signal-to-noise, only 150 signal counts are needed. Notice the total signal plus noise counts are nearly the same for all three figures while the total signal counts are quite different. This suggests that the single-particle photon bursts occur during a very short time, about 4×10^{-4} sec. in these cases. On the other hand, the clipped count gives a fairly good idea of the signal bursts.

In the absence of noise, a photon burst of two counts, one scattered from each beam, is in principle enough for a LTV speed measurement. However, even with clipping, some noise is present; ten signal counts is seen to be more than enough for a speed measurement in practice.

The sensitivity of photon burst correlation is clearly demonstrated. As a side issue, we point out that the second peak in Fig. 3(c) is seen to be taller than half of the first peak. This is due to the distortion caused by the process of clipping [17]. Although the shape of the correlation function may be distorted, the peak separation, and thus the measured speed, will not be altered by the process of single-clip correlation.

Figures 3(d) - 3(f) are correlation functions corresponding, respectively, to minimal detectable, noise, and good LDV speed measurements. Similar comments can be made for these figures. In general, the sensitivity of both methods are comparable; the measurement time used was the same for both experiments although the laser power for LDV measurements was a factor of two higher. Comparing Figs. 3(a), (b), (c) to Figs. 3(d), (e), (f), one observes without much surprise that the minimal clip count needed for a speed measurement is higher for LDV. However, once exceeding this minimal clip count, the sensitivity of single-particle LDV quickly improves and catches up with that of LTV.

Using the probability density mode of the digital correlator, the count distribution of photon bursts can be measured [9]. To demonstrate the usefulness of the count density distribution, we compared the photon bursts in a preset time interval resulting from scattering from a blackened paper to that from indoor natural aerosol; the results are shown in Figs. 4(a) and 4(b), respectively. The distribution of Fig. 4(a) is Poisson indicating the constant intensity of the sensing volume. The gradual tailing off of the distribution in Fig. 4(b) indicates the availability of large single particles, although with small probability.

The sample time for this experiment is chosen to be longer than the transit time of aerosol particles across the sensing volume [9].

IV. The Scaling Law and Performance Evaluation

The need for a figure of merit which takes into account the aerosol condition to evaluate the performance of laser velocimetry has been recognized, and the measurement rate was suggested as a logical choice in our early work [6]. With the photon-burst correlation technique, we have initiated [9] and more recently succeeded [10] in the formulation of a scaling law for laser velocimetry in visible wavelengths, relating the measurement rate of atmospheric crosswind due to individual particles, the signal particle arrival rate, F, to laser power P_o and measurement range, R, under a given aerosol condition. Although two laser beams are normally used in laser velocimetry, we used a single Gaussian-profiled beam with an e^{-2} radius, ρ, for the discussion of the scaling law. This is permissible since in a LDV setup, two beams are crossed into one spot containing intensity interference fringes, and in a LTV setup, most individual particles traverse both laser beams because the beam separation (typically $\sim$cm) is usually smaller than the characteristic length describing the turbulence of atmospheric wind field [10]. As a result, a single-beam arrangement should yield the same (or nearly the same) signal particle arrival rate (measurement rate), F. Using the concept of minimum detectable photon burst, n_s, and the associated power dependent minimum detectable particle radius, r_s, along with a generalized Junge distribution for the size distribution, $dN/dr = c_o r^{-\beta}$, the scaling law [10] for single particle arrival rate can be rewritten as

$$\frac{F}{\ell v \rho} = \frac{\sqrt{\pi}\, c_o}{(\beta-1)^{1.5}}\, r_s^{(1-\beta)} \qquad (2)$$

where

$$r_s = (n_s/\gamma)^{1/2}, \quad \gamma = \left(\sqrt{\frac{2}{\pi}}\,\frac{K_o A}{h\nu}\right)\frac{1}{v}\left(\frac{\eta P_o}{\rho R^2}\right),$$

and K_o, A, $h\nu$, v, η, ℓ, are, respectively, backscattering coefficient [6] ($\sigma = K_o r^2$), receiving telescope area, photon energy, crosswind speed, the efficiency of the detection system, and the depth of view. If during a measurement time, the correlator is set to accept photon bursts with photon counts exceeding the clip level, κ, at least m times, the minimum detectable photon burst [10] is

$$n_s = \sqrt{\frac{\pi}{2}}\,(\kappa + 1)\left(\frac{\rho}{v\tau_o}\right)\exp\left[\frac{1}{2}\left(\frac{v\tau_o}{\rho}\right)^2 (m - 1)^2\right] \qquad (3)$$

where τ_o is the sample time for the correlation. Typically, m is set to be the number of desired observable fringes in the sensing volume for LDV, and $m\tau_o$ approximates the width of the photon burst for LTV. It has also been shown mathematically [10] that using the probability mode of the digital correlator, the count distribution of photon burst, N(n), can be measured in a measurement time T_p, and that the signal particle arrival rate can also be obtained independently this way as,

$$F = \frac{1}{T_p}\int_{n_s}^{\infty} N(n)\,dn \qquad (4)$$

where

$$N(n) = \frac{\sqrt{\pi}\; c_o \ell v \rho T_p}{2(\beta-1)^{0.5}\gamma}\left(\frac{n}{\gamma}\right)^{-(\beta+1)/2}.$$

The correctness of the scaling law has been demonstrated in a laboratory experiment in which both signal particle arrival rate F and count distribution N(n) have been measured independently. The results are shown in Figs. 5 and 6. Both experiments give rise to the same value of β within the experimental error. The quantity $F/(\ell v \rho)$ in (2) can be interpreted as the number of particles per unit volume having radius greater than r_s, a quantity familiar to aerosol scientists [19]. When experimental conditions are such that a small range of r_s is encountered, the aerosol parameters c_o and β are constant and (2) may be used to determine these parameters experimentally. This was done previously in the laboratory [10] and together with the measured photon-count distribution, our scaling theory for performance evaluation of a laser time-of-flight velocimeter (LTV) was verified in a self-consistent manner.

However, when a large range of r_s is encountered, c_o and β may not be constant. In general, the measured value of β will increase as the aerosol radius increases. To obtain a wide range of r_s in our correlation experiments, the laser power P_o and beam radius ρ must be varied sufficiently. In this manner, the validity of (2) can be verified for a much wider range of r_s.

Following the same procedure outlined in Ref. 10 with a laser power P_o ranging from 0.3 mW to 0.4 W and beam radius ρ ranging from 40 to 900 μm by using different focussing lenses with R = 1.7 m and v = 5.2 m/sec, we have conducted extensive laboratory experiments covering r_s values from 0.1 to 4.0 μm. The experimental results when plotted as $F/(\ell v \rho)$ vs r_s is shown in Fig. 7. The resemblance of Fig. 7 to the typical cumulative number distribution of aerosols [19] is quite obvious. The β value changes from 3.2 to 6.1 as r_s increases in general agreement

with the expected room aerosol distribution. Our previous result of $\beta \simeq 4.3$ occurs at $r_s \simeq 1.5$ μm as a special case.

V. The Effect of Atmospheric Turbulence and Performance Prediction

In order to use (2) to predict the velocimetry performance, a realistic scaling law must first be established in the intermediate ranges from field experiments. The atmospheric aerosol condition is different, and the values c_o and β are expected to be different, from those obtained in the laboratory. Atmospheric turbulence should be monitored and its effect on the focussed beam radius, ρ, assessed. With the scaling law tested by the field experiments, the performance of the laser velocimeter at long ranges, such as 500 m can then be predicted.

It is well known that atmospheric turbulence, described by a constant denoting random refractive index fluctuations, C_n^2, produces undesirable effects of beam wander and beam breathing [20]. This reduces the visibility of intensity interference fringes in LDV operation [21]. In the summer of 1975 during our LDV field experiments [6], we also observed visually that although the interference fringes at a range of 1000 m, formed by unfocussed argon-ion laser beams, broke into patches, clear interference fringes could be seen within the patches for a time long enough for a photon-burst correlation measurement. The quantitative effect of turbulence on beam radius is still an open question. To our knowledge, among the vast amount of publications on atmospheric turbulence, only a few articles have addressed this question of beam radius directly. Fried [22] introduced the idea of optical resolution for imaging of a uniform circular beam through the atmosphere. His short exposure phase structure functions have been modified by Lutomirski et al [23], and Richardson [24] has used Fried's optical

resolution function to calculate beam radius. We have recently modified Fried/Richardson's formula for a Gaussian beam profile and made focussed beam radius measurements up to a range of 100 m using a photo-diode array. The experimental radii have been compared against three theoretical models of turbulence induced beam radius: Fried/Richardson's uniform circular beam [22,24] and the Gaussian beam models of Lutomirski et al [23] and of Kelley et al [25]. The detailed analysis and comparisons will be published elsewhere [25], but the main result is shown in Fig. 8. It is seen that the model of Kelley et al agrees with the experimental results better. The calculated beam radius at 500 m range for $C_n^2 = 10^{-13}$ $m^{-2/3}$, are $r_{TD} = 12{,}340$ μm, $r_{TC} = 12{,}860$ μm, $r_{TA} = 3{,}572$ μm, for the models of Fried/Richardson, Lutomirski et al, and Kelley et al, respectively. Again, the model of Kelley et al seems to agree with the observed focussed beam radius at 500 m, which when observable is about 0.5 cm, under the experimental conditions.

To establish the scaling law for field experiments, a set of single-beam experiments up to a range of 150 m have been made in the nights of summer 1982 and the signal particle arrival rates monitored by a computer. The atmospheric turbulence was simultaneously monitored by a NOAA C_n^2 meter [26]. The beam radii for the experimental conditions including measured C_n^2 were calculated with the three models described above along with a Gaussian diffraction model ignoring turbulence. The signal particle arrival rate F and minimum detectable particle radius, r_s, were determined from the experiment [10,25] and the data using the three sets of calculated ρ are fitted to (2). This procedure yields the best fitted aerosol parameters c_o and β, shown in Table I. Although the different

turbulence models predict quite different beam radii at high turbulence (see Fig. 8), their effects on the slope of the scaling law determined by β is seen to be minimal. This is due partly to the self-compensating nature of the turbulence effect on the signal strength (the total photon burst counts). The turbulence increases the beam radius at the sensing volume which decreases the laser intensity, but increases the transit time of the particle across the laser beam.

Over a period of two years, many sets of intermediate range field experiments were made [27,28] for the investigation of the scaling law, but only the experimental results of the summer 1982 were used for the determination of c_o and β, presented in Table I, because the values of C_n^2 were simultaneously recorded for these data. In addition, some single-beam measurements were made in the daytime up to a range of 100 m. For the daytime measurements, a narrow-band color filter (pass band $\sim$10 Å) was used in the receiver to reduce background light. Due to the background, the signal particle arrival rates are less than the rates at night for comparable ranges. At 25 m the arrival rate was found to be five-to-ten times lower.

In the summer and fall of 1982, night experiments were conducted at Fort Collins to measure the signal particle arrival rate at a range of 500 m with C_n^2 simultaneously monitored. Both single beam and dual beam experiments were conducted with about 0.25 W of laser power in the sensing volume. When two laser beams are used, the crosswind speed is determined by the ratio of beam separation to the measured time-of-flight. The effects of turbulence on the beam separation were investigated first by taking a home movie of two focussed laser spots at a range of 500 m. The fluctuations in beam separation were on the order

of 10%. Later, the beam separations were measured in the daytime for ranges of 100 m, 200 m, and 500 m in the atmosphere using a linear diode array. The fluctuation in beam separation was typically 5% for 100 m and 200 m range. At the 500 m range, the measured fluctuations of beam separation were from 2% to 15%, depending on the strength of the atmospheric turbulence.

The measured signal particle arrival rates F_m at 500 m are shown in Table II along with the predicted signal particle arrival rates and calculated minimum detectable particle radius based on the various turbulence models.

The usefulness of including turbulence in the calculation of signal particle arrival rate F and ρ is made clear by considering the first two experiments (7-20-1 and 7-20-2) of Table II. These are single beam experiments conducted a few days after the scaling law experiments in the summer of 1982. Predicted F for the Gaussian diffraction model is more than an order of magnitude below the measured rate F_m, while predicted F for the model of Kelley et. al. is comparable to F_m for these experiments. The predicted F for the other two turbulence models is comparable to F_m, but three to five times the predicted F for the model of Kelley et. al. The remaining two experiments conducted in the fall of 1982 used two beams. Predicted F, based on β and c_o from the summer 1982 scaling law experiments, is comparable to F_m for all the models considered. What is perhaps more important is that the model of Kelley et. al. gives the most reasonable minimum detectable particle radius among all models considered. Considering the infrequency of the signal events (100-600 sec. per acceptance) at the range of 500 m, the agreement between theory and experiment is quite good.

VI. The Prospect of Routine Long-Range Operation

As mentioned in the Introduction, it is the general conclusion of researchers [2,5,8,16] that long-range (500-1000 m) wind speed measurements using cw visible lasers should be possible on a routine basis. Nonetheless, routine operations at these ranges have not yet been realized. Although the measurements at 500 m reported here have clearly demonstrated the possibility and feasibility of wind speed measurements in the visible at long ranges with cw lasers, the signal particle arrival (measurement) rate is still too low to be of practical and routine use.

To further improve the performance and increase the measurement rate, higher laser power should be used. In addition, different methods for signal analysis which can handle photon bursts resulting from scattering of multiple particles should be investigated as well. Although the theoretical and experimental measurement rates at the range of 500 m were comparable, the calculated minimum detectable signal particle radius r_s ($\sim$ 200 μm), is too large to be abundant enough in normal clear air. The accepted measurements at 500 m may be partially due to several particles moving across the laser beam together. A typical correlation function probably resulting from more than one particle at 500 m under clear air conditions is shown in Fig. 9(a). This is compared to a correlation function resulting presumably from a single particle crossing the laser beams at the same range in a drizzle with higher wind as shown in Fig. 9(b). The presence of multiple-particle signals at long ranges is unavoidable and the measurement rate can be greatly increased, if these signals can be accepted in a recognizable form. In this respect, the LDV measurement using a fast Fourier

transform method [16] which analyzes the frequency instead of the intensity of a photon burst, may be more suitable. In fact, Durst and Richter have recently been able [29] to conduct routine wind-speed measurements at a range of 350 m. Proper processing of LTV correlation functions as a part of the acceptance criteria using some curve-fitting procedure to enhance the double humps should also facilitate LTV measurements at long ranges.

In summary, this report reviews the photon-burst correlation techniques of LDV and LTV for atmospheric crosswind measurements using cw lasers at visible wavelengths. Measurements based on photon bursts resulting from individual signal particles can be readily made up to a range of a few hundred meters; their measurement rates can be understood by a theory, including the effect of turbulence, presented herein. Experimental evidences of successful crosswind measurements up to 500 m suggest that signal resulting from multiple particles at long ranges can no longer be ignored. In addition to the use of higher power lasers [16,30], proper use of this type of signal and its inclusion in the data analysis will increase the measurement rate at long ranges (up to 1000 m) and should make laser velocimetry good enough for routine atmospheric applications.

Acknowledgements

The authors wish to thank K. G. Bartlett, L. S. Hsu, and H. Shimizu for their valuable contributions, and thank W. A. Flood and M. B. Richardson for discussions.

References

1. Y. Yeh and H. Z. Cummins, Appl. Phys. Lett. 4, 176 (1964).

2. L. Danielsson and E. R. Pike, J. Phys. E 16, 107 (1983), and references therein.

3. 2nd Topical Meeting on Coherent Laser Radar: Technology and Applications, Technical Digest (Optical Society of America, 1983). The meeting was held in Aspen, Colorado, August 1-4, 1983; the concept of WINDSAT and its hardware developments were discussed extensively.

4. M. J. Post, F. F. Hall, R. A. Richter, and T. R. Lawrence, Appl. Opt. 21, 2442 (1982).

5. E. O. Schulz-DuBois, ed., Photon Correlation Techniques in Fluid Mechanics, (Springer-Verlag, 1983). This is the proceedings of the 5th international conference held at Kiel-Damp, F.R.G., May 23-26, 1982; most of the active research groups in atmospheric cross-wind sensing using photon-correlation techniques were represented.

6. K. G. Bartlett and C. Y. She, Appl. Opt. 15, 1980 (1976).

7. K. G. Bartlett and C. Y. She, Opt. Lett. 1, 175 (1977).

8. C. Y. She, Opt. Acta 26, 645 (1979).

9. K. G. Bartlett and C. Y. She, J. Opt. Soc. Am. 69, 455 (1979).

10. C. Y. She and R. F. Kelley, J. Opt. Soc. Am. 72, 365 (1982).

11. P. J. Bourke and C. G. Brown, Optics and Laser Tech. 4, 23 (1971).

12. W. M. Farmer and J. O. Hornkohl, Appl. Opt. 12, 2636 (1973).

13. L. Danielsson, in Proceedings of the Symposium on Long Range and Short Range Optical Velocity Measurements, H. J. Pfeiffer, ed., Report ISLR 117/80, paper XII, (1980).

14. F. Durst, B. Howe, and G. Richter, in Photon Correlation Techniques in Fluid Mechanics, W. T. Mayo, Jr. and A. E. Smart, ed., Stanford Joint Institute for Aeronautics and Acoustics publication, paper 3 (1980).

15. L. Lading, A. Skov-Jensen, C. Fog, and H. Andersen, Appl. Opt. 17, 1486 (1978).

16. F. Durst, B. M. Howe, and G. Richter, Appl. Opt. 21, 2596 (1982).

17. J. B. Abbiss, in Photon Correlation Techniques in Fluid Dynamics, E. O. Schulz-DuBois, ed., p. 30, (Springer-Verlag, 1983).

18. M. Kerker, The Scattering of Light and Other Electromagnetic Radiation, (Academic Press, 1969).

19. S. Twomey, Atmospheric Aerosols, (Elsevier, Amsterdam, 1977), p. 9.

20. R. L. Fante, Proc. IEEE 63, 1669 (1975).

21. H. J. Pfeifer, M. König, and B. Koch, J. Opt. Soc. Am. 70, 163 (1980).

22. D. L. Fried, J. Opt. Soc. Am. 56, 1372 (1966).

23. R. F. Lutomirski, W. L. Woodie, and R. G. Buser, Appl. Opt. 16, 665 (1977).

24. M. B. Richardson, A General Algorithm for the Calculation of Laser Beam Spreading, ASL-TR-0116, U.S. Army Atmospheric Sciences Laboratory, White Sands Missile Range, NM (1982).

25. R. F. Kelley, L. S. Hsu, and C. Y. She, submitted to J. Opt. Soc. Am. for publication.

26. G. R. Ochs, W. D. Cartwright, and D. D. Russell, Optical C_n^2 Instrument Model II, NOAA Technical Memorandum ERL WPL-51 (1979).

27. R. F. Kelley, Performance Evaluation and Estimation of a Laser Time-of-Flight Velocimeter, Ph.D. thesis, (Colorado State University, 1983) (unpublished).

28. R. F. Kelley, L. S. Hsu, H. Shimizu, and C. Y. She, in Photon Correlation Techniques in Fluid Dynamics, E. O. Schulz-DuBois, ed., p. 205 (Springer-Verlag, 1983).

29. H. J. Pfeifer and E. Sommer, private communication.

30. E. Sommer and H. J. Pfeifer, in 2nd Topical Meeting on Coherent Laser Radar: Technology and Applications, Technical Digest, Paper WAII, (Optical Society of America, 1983).

Table I. Aerosol distribution constants c_o and β as determined from the scaling law.

Model	c_o	β
Fried/Richardson[a)]	2.83×10^{-8}	3.19 ± 0.17
Lutomirski et al[b)]	1.60×10^{-8}	3.25 ± 0.18
Kelley et al[c)]	5.04×10^{-10}	3.47 ± 0.20
Gaussian Diffraction[d)]	1.48×10^{-10}	3.55 ± 0.21

From Ref. 25, [a)]The uniform circular model, r_{TD}, [b)]The Gaussian model of Lutomirski et al, r_{TC}, [c)]The modified Gaussian model, r_{TA}, and [d)]The diffraction model, r_C.

Table II. Experimental results at a 500 m range.

			Predicted F and r_s for Radius ρ							
			$\rho = r_G$		$\rho = r_{TA}$		$\rho = r_{TC}$		$\rho = r_{TD}$	
Exp	N	F_m (#/sec)	r_s (μm)	F (#/sec)	r_s (μm)	F (#/sec)	r_s (μm)	F (#/sec)	r_s (μm)	F (#/sec)
7-20-1	12.65	1.0×10^{-2}	555	2.85×10^{-4}	222	9.12×10^{-3}	528	3.77×10^{-2}	503	4.67×10^{-2}
7-20-2	13.0	5.25×10^{-2}	174	3.80×10^{-3}	144	1.52×10^{-2}	319	4.84×10^{-2}	308	5.73×10^{-2}
10-6-1	13.25	3.0×10^{-3}	155	1.17×10^{-3}	195	1.49×10^{-3}	555	2.26×10^{-3}	532	2.80×10^{-3}
11-29-1	12.75	1.67×10^{-3}	61.0	4.80×10^{-3}	97.9	3.96×10^{-3}	449	2.84×10^{-3}	427	3.50×10^{-3}

N is the exponent in the refractive index structure constant $C_n^2 = 10^{-N} m^{-2/3}$, and r_G, r_{TA}, r_{TC}, and r_{TD} are calculated beam radius using different models defined for Table I. F_m is the measured signal particle arrival rate, F is the predicted arrival rate, and r_s is the calculated minimum detectable particle radius.

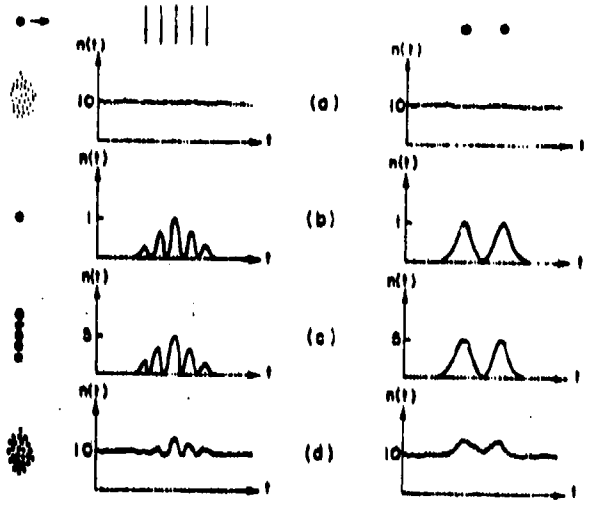

Fig. 1. The intensity n(t) resulting from the scattering of (a) many small particles, (b) one single particle, (c) five signal particles simultaneously traversing the sensing volume, and (d) 20 randomly distributed signal particles.

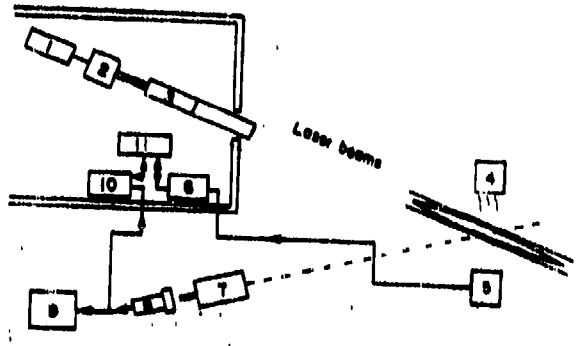

Fig. 2. Expermental arrangement for LTV measurements. 1. Laser, 2. beam splitter, 3. focussing telescope, 4. fan, 5. cup anemometer, 6. anemometer electronics, 7. receiving telescope, 8. photomultiplier assembly, 9. digital rate meter, 10. digital correlator, and 11. computer. The fan is used only in the laboratory experiments to generate the wind.

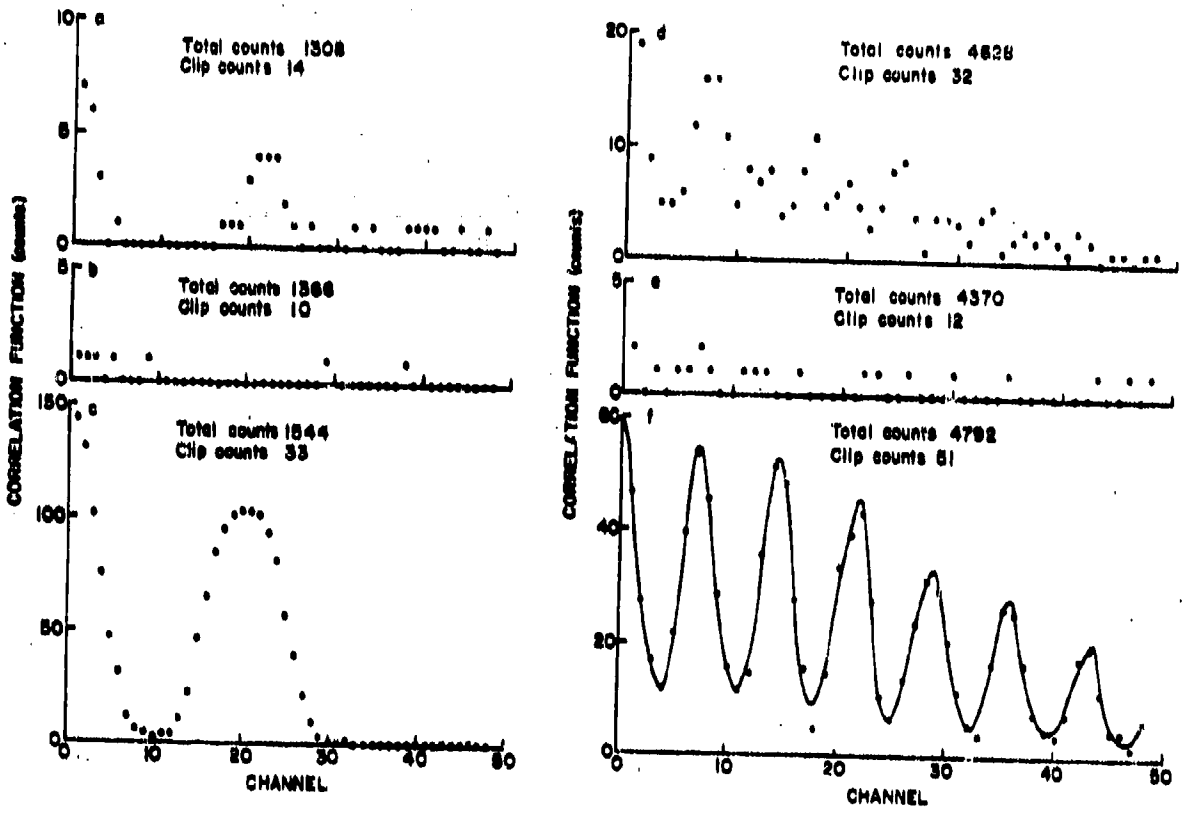

Fig. 3. Selected correlation functions, three for LTV and three for LDV, for demonstrating the sensitivity of photon burst correlation for velocity measurements. The power used in (d), (e), (f) is a factor of two higher than that used in (a), (b), (c). The total measurement time is two sec. each: 10^5 samples with 20 μsec/sample(channel) for LTV and 10^6 sample with 2 μsec/sample(channel) for LDV.

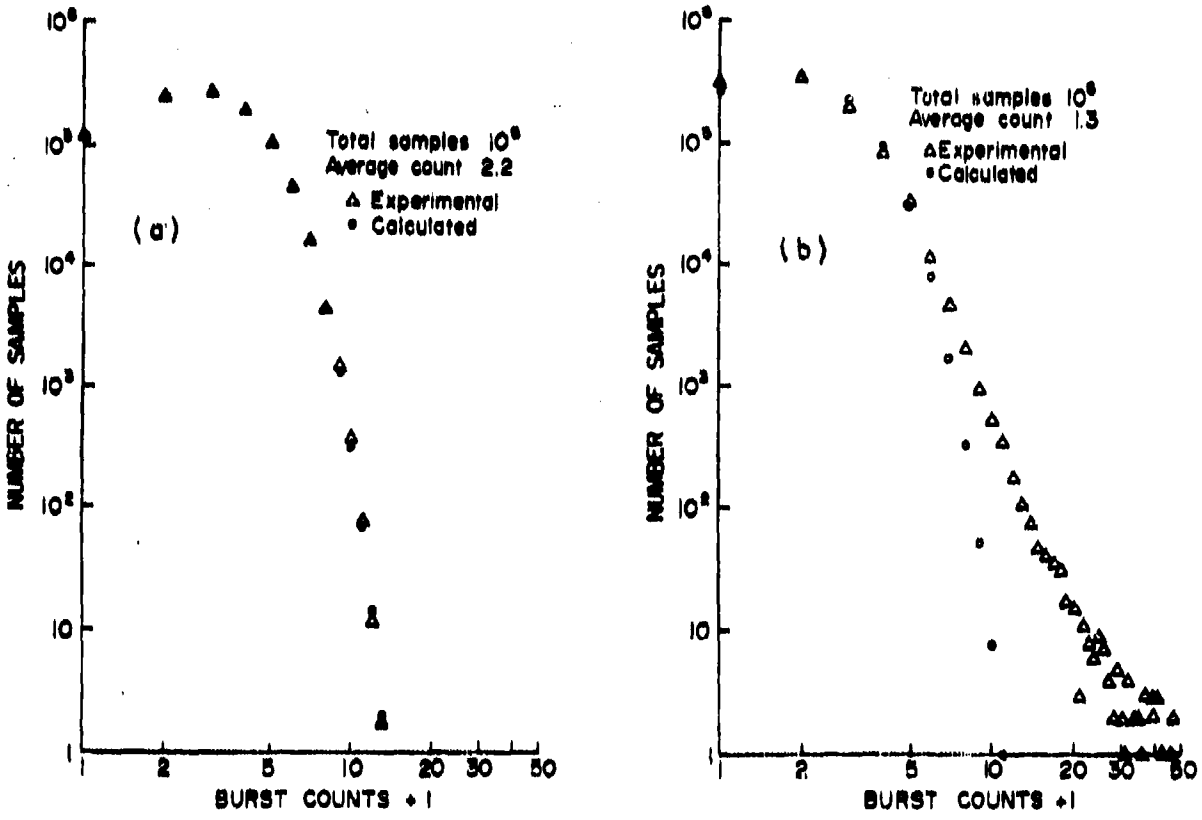

Fig. 4. Probability density of burst counts from a uniformly illuminated target (a) and indoor natural aerosol (b).

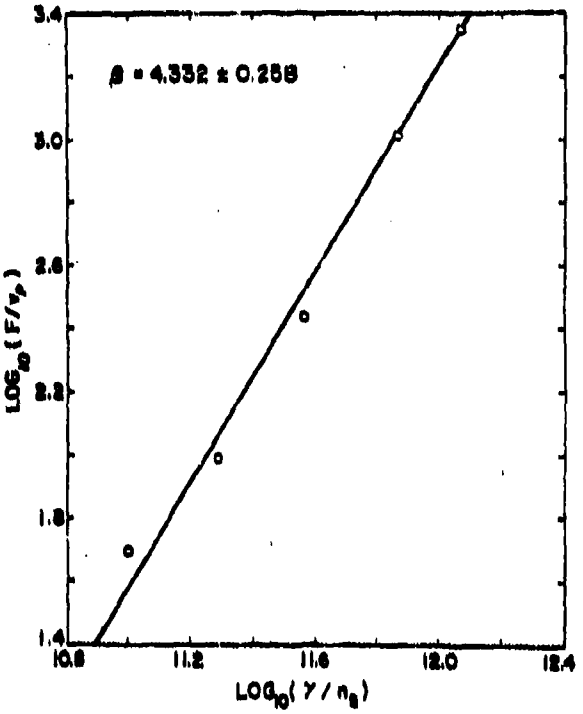

Fig. 5. Scaling law of the laboratory correlation experiment. The LTV measurement rate F is plotted as a function of experimental parameters, such as laser power P_0 and detector range R. The slope of this plot yields the power of the aerosol-size distribution, $\beta = 4.332 \pm 0.258$.

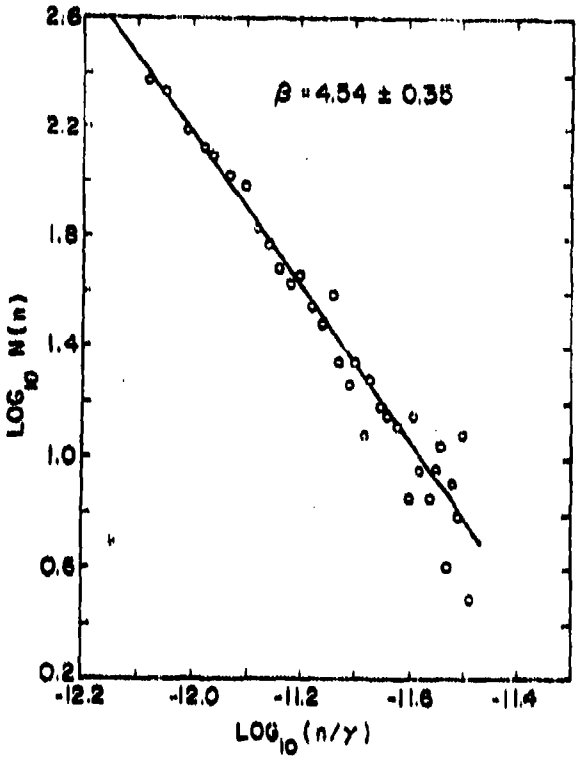

Fig. 6. Photon-count distribution N(n) of signal particles plotted as a function of photon counts per sample n divided by γ, which contains experimental parameters. The slope of the plot yields the power of the aerosol size distribution, $\beta = 4.54 \pm 0.35$.

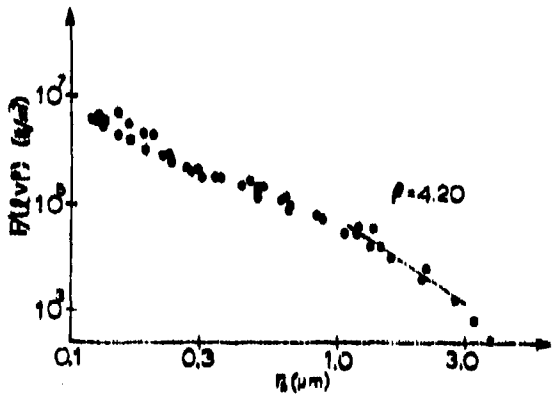

Fig. 7. Scaling law of the laboratory experiments over a wide range of r_s. The LTV measurement rate F divided by ($\ell v \rho$) is plotted as a function of minimum detectable radius r_s which depends on experimental parameters such as laser power P_o and detection efficiency η. With the wide range of r_s (0.1-4 μm) covered, the slope of this plot yields varied values for the power of the aerosol-size distribution, β = 3.2-6.1.

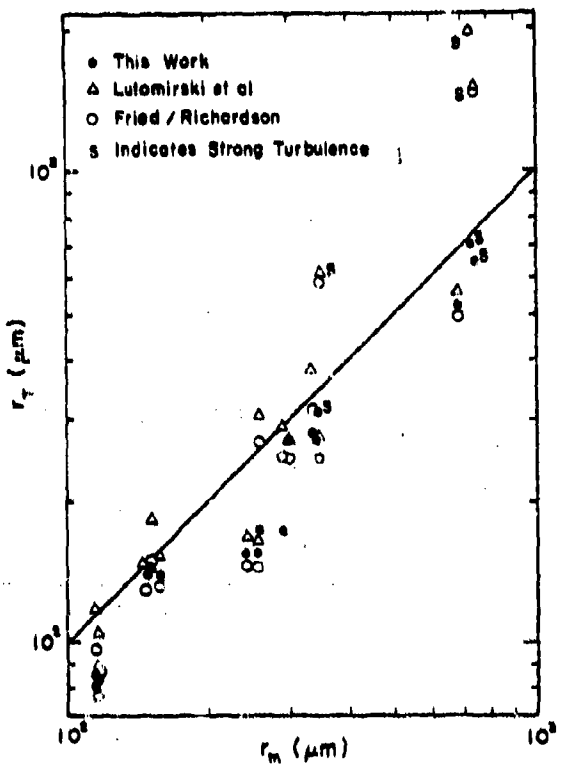

Fig. 8. Measured e^{-2} beam radius, r_m, vs predicted beam radii, r_T, for three turbulence models.

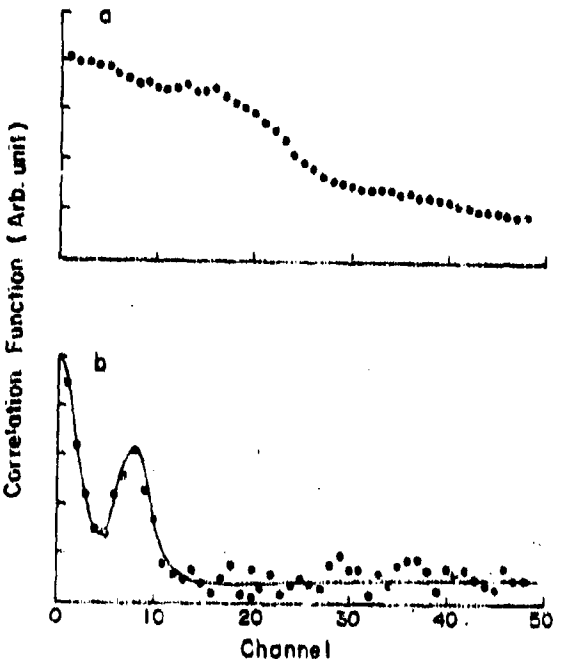

Fig. 9. Measured photon-burst correlation functions at 500 m under different atmospheric conditions: (a) in clear air due possibly to several particles, and (b) in drizzle due possibly to a single light rain drop, scattering from the two laser beams. The sample time τ_o (per channel) is 1.0 msec. The beam separation is 1.9 cm and 3.4 cm for (a) and (b), respectively.